

# Self-reproducing micelles coupled to a secondary catalyst

Elias Post, Andrew J. Bissette and Stephen P. Fletcher\*

 Received 00th January 20xx,  
Accepted 00th January 20xx

DOI: 10.1039/x0xx00000x

www.rsc.org/

We report a physical autocatalytic system where micelles self-reproduce via a copper-catalyzed azide-alkyne cycloaddition in a biphasic reaction mixture. The coupling of a secondary catalyst to an autocatalytic cycle opens up new opportunities to control and probe autocatalytic processes.

Physical autocatalysis, the chemical self-reproduction of micelles and vesicles, offers an experimental model of the growth and division of biological compartments. Such systems have been used to model homeostasis and to drive the growth and division of synthetic protocells.<sup>1–3</sup> In physical autocatalytic processes surfactants are formed at the interface of a biphasic system, for example, by hydrolysis of a hydrophobic ester to produce a fatty acid<sup>4</sup> or by the reaction between hydrophobic and hydrophilic components to form an amphiphile (Fig. 1, A).<sup>5</sup> Once a critical concentration of the products is reached, aggregates such as micelles and vesicles form. These aggregates allow reaction components to mix by encapsulating them and transporting them to a different phase, facilitating further surfactant formation, and are therefore self-reproducing.<sup>6</sup> Self-reproduction is fundamental to any living system and physical autocatalytic processes have been proposed as minimal metabolic networks where compartmentalized reactions generate self-organizing components of the compartment.<sup>7,8</sup>

Physical autocatalysis has to date largely relied on a narrow set of reactions,<sup>4,6,9,10</sup> and in particular the coupling of surfactant self-reproduction to a secondary catalytic cycle is poorly explored.<sup>11</sup> The use of a secondary catalyst in an autocatalytic cycle would be expected to show much different behaviour than autocatalysis driven by spontaneous reactions and may offer opportunities to control the properties of autocatalytic system in ways that would not otherwise be possible.

Copper-catalyzed azide-alkyne cycloaddition (CuAAC) is a promising candidate for coupling physical autocatalysis

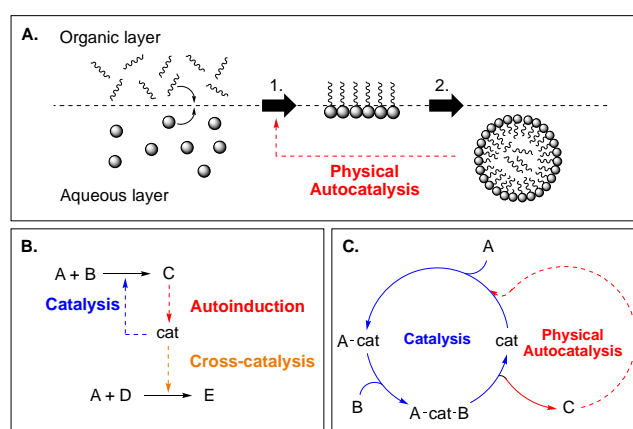


**Fig. 1** A. Overview of the mechanism of physical autocatalysis. B. A network where an autoinductive reaction forms a ligand and has a cross-catalytic relationship with a lipid forming reaction (Devaraj, 2015). C. This work: product micelles accelerate the formation of a catalytic intermediate.

to a secondary catalyst. It is water tolerant and a wide range of modular ligands can be used to stabilize the copper catalyst, offering opportunities to tune its properties and hence the overall kinetics of the reaction. This approach also promises to be highly modular, once working conditions are found. The polar headgroup or hydrophobic tails could be easily varied without disturbing the mechanism of the autocatalytic reaction.

CuAAC conditions have previously been applied by Devaraj in a system where membrane bound copper catalysts synthesize their own ligand and a membrane forming lipid (Fig. 1, B).<sup>12</sup> They also used these CuAAC reactions to form self-replicating nano-scale peptide aggregates.<sup>13</sup> Both of these reactions are autoinductive with respect to the copper catalyst: it promotes the formation of a ligand, which binds to the catalyst and increases its efficiency.<sup>14</sup>

Here we report a CuAAC based physical autocatalytic system where a micelle functions as a phase transfer catalyst and allows phase separated compounds to react. (Fig. 1, C) We designed an autocatalytic reaction in which hydrophilic maltose azide **1** dissolved in the water phase reacts with

\* Department of Chemistry, Chemistry Research Laboratory, University of Oxford, 12 Mansfield Road, Oxford, OX1 3TA, U.K.

† Electronic Supplementary Information (ESI) available: [details of any supplementary information available should be included here]. See

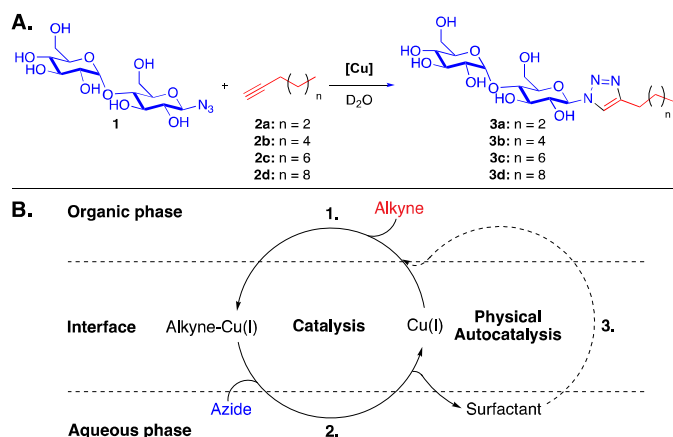


**Fig. 2.** A. The reaction performed in the reported autocatalytic system, where maltose azide **1** is coupled to alkynes **2a-d** of various chain lengths via a CuAAC reaction to form surfactants **3a-d**. B. Our working model of the catalytic cycle operating in tandem with a physical autocatalytic cycle.

hydrophobic aliphatic alkyne **2** that constitutes the organic phase via a CuAAC reaction to form surfactant **3** (Fig. 2, A). We synthesised a series of surfactant products, varying in the length of the hydrophobic tail. DLS and fluorimetry measurements demonstrated that they form nanometre-size micelles at millimolar concentrations (Fig. S13-S18). Surfactants with shorter chain lengths have higher CMCs and for compound **3a** no aggregation was observed. Reactions involving alkyne **2a** can therefore be taken as control reactions

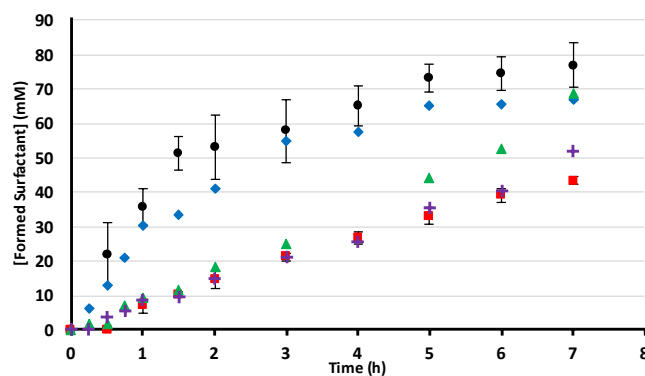


**Fig. 3.** Summary of kinetic studies on a CuAAC reaction with *O*-phenylenediamine as a ligand and **1** and **2c** as coupling partners. The reaction is monitored by consumption of azide **1** and formation of surfactant **3c** by  $^1\text{H}$  NMR spectroscopy. Points are the mean of three independent experiments and the error bars are the standard deviation. Unseeded reaction (red squares): **1** (150 mg, 91 mM) and **2c** (150  $\mu\text{L}$ , 0.83 mmol, 2 eqv) are stirred at 200 rpm with  $\text{CuSO}_4 \cdot 5\text{H}_2\text{O}$  (6 mg, 5.3 mM), *O*-phenylenediamine (6.6 mg, 13.6 mM) and sodium ascorbate (18.2 mM) in  $\text{D}_2\text{O}$  (4.5 mL). A lag period of half an hour followed by a faster reaction period is observed. Seeded reactions: when the reaction is seeded with surfactant **3c** (22 mM for black circles, 12.8 mM for blue diamonds, 3.4 mM for green triangles and 1.4 mM for purple pluses) at  $t = 0$  above the CMC (2.86 mM) the lag period is eliminated and the reaction proceeds at a faster rate. Higher concentrations of seeding lead to a more pronounced increase in the rate of product formation.

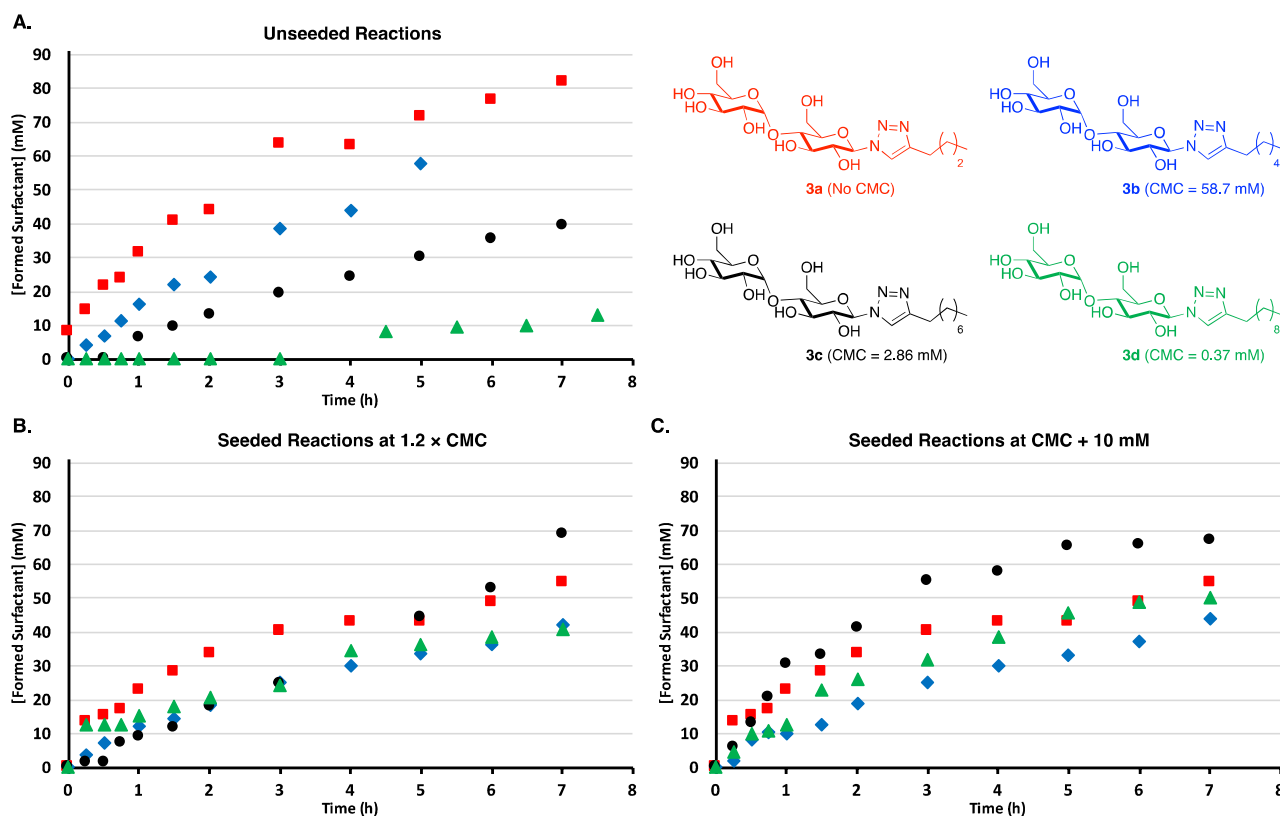


**Fig. 4.** A. Kinetic profile for unseeded reactions using **1** and different chain length alkynes **2a-d** as coupling partners. A clear trend between the chain length and reaction rates is observed; **2a** (red squares), **2b** (blue diamonds), **2c** (black circles) and **2d** (green triangles). B. Kinetic profile for seeded reactions at 1.2 times the CMC; seeded with 80 mM of **3a** (red squares), 70.4 mM of **3b** (blue diamonds), 3.40 mM of **3c** (black circles) and 0.44 mM of **3d** (green triangles). C. Kinetic profile for seeded reactions at the CMC plus 10 mM; seeded with 80.0 mM of **3a** (red squares), 68.7 mM of **3b** (blue diamonds), 12.8 mM of **3c** (black circles) and 10.4 mM of **3d** (green triangles).

where physical autocatalysis can not readily occur.

Conventional aqueous CuAAC reaction conditions, namely in situ reduction of CuSO<sub>4</sub> with sodium ascorbate, gave unreliable results and catalyst deactivation. We found that using *O*-phenylenediamine and CuSO<sub>4</sub>·5H<sub>2</sub>O provided reproducible kinetic behaviour and stabilised the copper towards oxidation.<sup>15</sup> Kinetic study of the reaction between azide **1** and alkyne **2c** revealed a lag period followed by subsequent rate acceleration (Fig. 3, red squares). Seeding the reaction at *t* = 0 with product **3c** above the CMC (2.86 mM) removed the lag period and increased the rate of product formation. These observations are consistent with an autocatalytic mechanism.<sup>14</sup> Consistent with previous studies, minor variations in stirring rate and concentration and even the position of the flask above the stirring plate affected the duration of the lag period and overall reaction time.<sup>5</sup> This sensitivity to physical parameters leads to some variability between independent repeats but the overall trends are reproducible.

When the reaction was seeded at *t* = 0 with **3c** at concentrations close to the CMC (Fig. 3, 1.4 mM for purple crosses and 3.4 mM for green triangles) an increase in the rate of product formation only became apparent at later time points. Seeding at a higher concentration (12.8 mM for blue diamonds) led to a significant rate increase, but the autocatalytic effect appears to saturate as a final experiment at 22 mM (black circles) showed no significant further increase in rate. The unseeded reaction never reaches the rate of product formation observed during the seeded reactions, possibly because a significant amount of starting material is consumed by the time a comparable concentration of product has been generated.<sup>11</sup> Varying the chain length of the hydrophobic alkynes revealed a negative correlation, where longer chains had lower reaction rates and longer lag periods. (Fig. 4, A). This could be ascribed to their decreased solubility in the aqueous layer (0.36 mg/mL for **2a** while it is 0.024 mg/mL for **2b**) which leads to increased lag periods even though surfactants with longer chain lengths have lower CMCs.<sup>16</sup>

Two different systematic approaches to the degree of seeding were applied where in one case all the reactions were

seeded at 1.2 times the CMC (Fig. 4, B) in the other case reactions were seeded at the CMC plus 10 mM (Fig. 4, C). Since **3a** does not have a CMC the reaction was seeded with an arbitrary amount of 80 mM. This approach resulted in a much higher concentration of seeding for **3a** and **3b** compared to **3c** and **3d**, and seeding at >50 mM concentrations actually leads to reaction inhibition for **3a** and **3b** as they formed at significantly slower rates than their unseeded counter parts. When the reaction was seeded below the CMC with 36 mM of **3b** rate acceleration is still observed when about 20 mM of additional product had formed (Fig. S27). Triazoles are known ligands for copper, so at higher concentrations the product could start to inhibitably bind to the copper.<sup>17</sup> When non-surfactant maltose triazole **3e**, synthesized from propargyl alcohol and **1** (See SI) was added to a reaction between **1** and **2a** (Fig. S26) inhibition was also observed.

Longer chain surfactants **3c** and **3d** behave differently under seeded conditions. When seeded at 1.2 times the CMC the lag periods were removed but there was only a minimal increase in the rate of product formation. However, when the CMC plus 10 mM conditions were applied a more significant increase in the rate of product formation was observed, and the longer tail compounds benefit much more from seeding than **3a** and **3b**.

We probed the phase behaviour of the reaction components using diffusion ordered spectroscopy (DOSY). Control experiments confirmed that our surfactants aggregate above their CMCs. The alkyne is fully associated with the surfactant **3c** above its CMC, while azide **1** on the other hand is not detectably associated (Fig. 5, Table S1). The water-soluble copper-ligand complex diffuses at a slower rate than the free ligand indicating copper coordination. This complex does however not appear to associate with the micelle.

Next, the reaction was performed in a 1:1 water/*tert*-butanol mixture to facilitate phase mixing.<sup>8</sup> Here the lag period was eliminated and the reaction was complete within 1.5 hours (Fig. S24) but the reaction still had a sigmoidal rate profile. Repeating the reaction under seeded conditions removed the sigmoidal profile and the reaction time remained at 1.5 hours. These results are consistent with the idea that phase behaviour is responsible for the lag period and slower

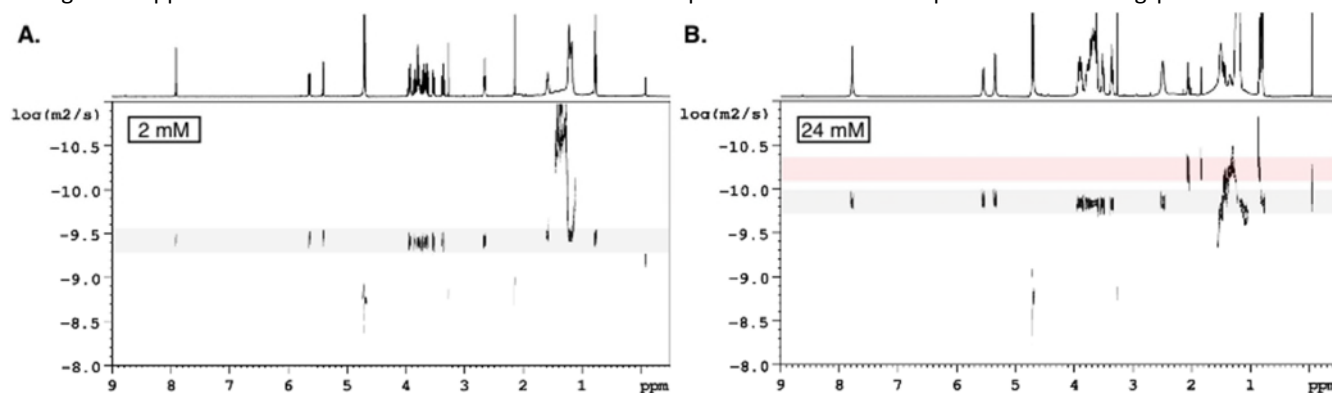


**Fig. 5** 2D-DOSY spectra at surfactant **3c** (*n* = 6) concentration of 2 mM (**A**) below and 24 mM (**B**) above the CMC (3 mM) in the presence of **2c**. The x-axis represents the chemical shift in ppm while the y-axis represents the diffusion rate in log(m<sup>2</sup>/s). The diffusion rate for the surfactant is highlighted in grey and while the rate for **2c** is highlighted in red. At a concentration below the CMC the surfactant diffuses at a fast rate and **2c** does not appear to dissolve. However, at a higher concentration when micelles are present the surfactant diffuses at a slower rate and **2c** appears to be highly associated with the micelles by diffusing at an even slower rate.

kinetics observed under autocatalytic conditions.

The mechanism by which physical autocatalysis occurs in related biphasic micellar systems is proposed by Luisi and coworkers to be predominantly due to micellar catalysis.<sup>4</sup> However Buhse and coworkers interpreted such physical autocatalytic processes as being mainly a form of phase transfer catalysis.<sup>18,19</sup> The key difference of the two models is where the reaction takes place: Luisi *et al.* suppose the reaction occurs within the micelle interior while Buhse *et al.* propose reactions happen in the aqueous phase after dissociation of a precursor-surfactant complex.

In the system reported here, rate acceleration is only observed when the product concentration exceeds the CMC. This suggests micelles are necessary for autocatalysis, but whether a micellar mechanism or a phase transfer mechanism (or both mechanisms) operates is not clear from these experiments. The strong alkyne–micelle association observed by DOSY is consistent with micellar catalysis, however, where exactly the reaction takes place is not obvious. If alkyne diffuses from the micelle into water before it reacts a phase transfer mechanism is at play. On the other hand, for explicit micellar catalysis to occur polar **1** and the copper–ligand complex should diffuse into the micelles which was not observed by DOSY.

Our current mechanistic hypothesis is shown in Fig. 2B. First the organic alkyne encounters the aqueous copper catalyst at the interface which is likely to be the rate limiting step (Fig. 2, step 1). Once the copper–alkyne complex has formed it has to coordinate to the aqueous azide but since the complex is more water soluble this step should proceed more readily (step 2). After demetallation the copper–ligand complex reenters the catalytic cycle while the surfactant will eventually form micelles once the CMC is reached. These micelles can then drastically speed up the first step by facilitating the interaction between the alkyne and the copper catalyst thereby driving the autocatalytic cycle (step 3).

We have developed a new autocatalytic reaction driven by CuAAC that promises to be highly modular in nature. The presence of a secondary catalyst which can interact with the autocatalyst based on the properties of its ligand offers a potential handle to tune the kinetics of the overall system.

Further study of this system is underway in our lab. We anticipate that simple, rational variations in catalyst structure will offer a straightforward method for controlling the reaction and may provide mechanistic insight. We anticipate that these studies might prove useful in understanding how control over the spatial organisation of compartmentalized reactions may be used to drive different reaction outcomes.

## Conflicts of interest

There are no conflicts to declare.

## Notes and references

‡ We thank the European Research Council (Consolidator Grant ‘autocat’, 681491) and the EPSRC (Standard Grant EP/M025241/1) for funding.

¶ A seeded reaction at 22 mM was repeated but with the concentration of starting materials **1** and **2c** decreased by 22 mM (Fig. S25). Surprisingly, this led to a similar rate of initial product formation as the original seeded reaction. There may be a difference in autocatalytic efficiency between product manually added and generated in situ but, if so, why is currently unclear.

£ Under these conditions **2c** was completely dissolved, however, upon addition of copper and ligand phase separation occurred leading to inhomogeneity.

- 1 H. H. Zepik, E. Blöchliger and P. L. Luisi, *Angew. Chemie - Int. Ed.*, 2001, **40**, 199–202.
- 2 K. Kurihara, M. Tamura, K. Shohda, T. Toyota, K. Suzuki and T. Sugawara, *Nat. Chem.*, 2011, **3**, 775–781.
- 3 J. W. Szostak, D. P. Bartel and P. L. Luisi, *Nature*, 2001, **409**, 387–390.
- 4 P. A. Bachmann, P. L. Luisi and J. Lang, *Nature*, 1992, **357**, 57–59.
- 5 A. J. Bissette, B. Odell and S. P. Fletcher, *Nat. Commun.*, 2014, **5**, 4607.
- 6 P. Stano and P. L. Luisi, *Chem. Commun.*, 2010, **46**, 3639–3653.
- 7 F. G. Varela, H. R. Maturana and R. Uribe, *BioSystems*, 1974, **5**, 187–196.
- 8 P. L. Luisi, *Naturwissenschaften*, 2003, **90**, 49–59.
- 9 A. J. Bissette and S. P. Fletcher, *Angew. Chemie - Int. Ed.*, 2013, **52**, 12800–12826.
- 10 K. Ruiz-Mirazo, C. Briones and A. De La Escosura, *Chem. Rev.*, 2014, **114**, 285–366.
- 11 K. Takakura, T. Toyota and T. Sugawara, *J. Am. Chem. Soc.*, 2003, **125**, 8134–8140.
- 12 M. D. Hardy, J. Yang, J. Selimkhanov, C. M. Cole, L. S. Tsimring and N. K. Devaraj, *Proc. Natl. Acad. Sci.*, 2015, **112**, 8187–8192.
- 13 R. J. Brea and N. K. Devaraj, *Nat. Commun.*, 2017, **8**, 730.
- 14 D. G. Blackmond, *Angew. Chemie Int. Ed.*, 2009, **48**, 386–390.
- 15 A. Baron, Y. Blériot, M. Sollogoub and B. Vauzeilles, *Org. Biomol. Chem.*, 2008, **6**, 1898.
- 16 C. McAuliffe, *J. Phys. Chem.*, 1966, **70**, 1267–1275.
- 17 T. R. Chan, R. Hilgraf, K. B. Sharpless and V. V. Fokin, 2004, **41**, 2002–2004.
- 18 T. Buhse, R. Nagarajan, D. Lavabre and J. C. Micheau, *J. Phys. Chem. A*, 1997, **101**, 3910–3917.
- 19 T. Buhse, D. Lavabre, R. Nagarajan and J. C. Micheau, *J. Phys. Chem. A*, 1998, **102**, 10552–10559.